USING TSUNAMI INTERFEROMETRY TO DETECT THE KUROSHIO CURRENT

Soham Bhattacharya, Jadavpur University
Supervisor: Shingo Watada

ABSTRACT

Cross-correlation techniques have long been used for ambient noise tomography where the cross-correlation functions are mathematically treated to obtain phase and group speed maps which then offer information about internal structures of the Earth. The construction of cross-correlation functions allowed seismologists to use ambient noise, which was previously considered worthless, to simulate virtual seismic sources, i.e, earthquakes travelling from one station to the other, with each station acting as a source for the other depending on the time domain under consideration. Seismologists no longer have to wait for real earthquakes events for data to study the internal structure of the Earth.

In our study, we apply the technique of cross-correlations on data procured from the network of deep ocean pressure sensors, DONET (Dense Oceanfloor Network system for Earthquakes and Tsunamis) and try to detect the Kuroshio current travelling over these sensors.

1. INTRODUCTION

The fact that information about internal structure of the Earth could be derived from ambient seismic noise was first demonstrated by Shapiro and Campillo in 2004[1]. They calculated and stacked cross correlations of around a month of data across several station pairs separated from each other by a few hundred kilometers to thousand kilometers. The cross-correlation functions gave rise to dispersive waveforms which had velocities consistent with those predicted from the global Rayleigh-wave tomographic maps. The results of Shapiro and Campillo showed that coherent Rayleigh waves can be extracted from the ambient seismic noise and that their dispersion characteristics can be accurately determined. This provided a new source for Earth tomography without waiting for an earthquake. The station pairs act like virtual earthquake sources for each other. Travel time of waves from one station to the other gave a measure of prevailing wave speeds.

Cross-correlation of seismic waves has several other applications like detection of oil reserve cavities without using explosives or destructive methods[2].

In our study, we compute the cross-correlation from deep ocean pressure sensors to simulate virtual tsunami waves travelling from one station to the other and calculate phase speeds. A direction dependency of the phase speeds of the virtual tsunami waves is due to

superimposed strong ocean current on the virtual tsunami waves simulated by the cross-correlations and this is indicated by the change in expected travel time from one station to the other.

2. THE KUROSHIO CURRENT

The Kuroshio current, alternatively known as the Black or Japan Current, is a warm, northward-flowing oceanic current located on the western periphery of the North Pacific Ocean basin, along the east coast of Japan. The Kuroshio is a strong western boundary current, transporting tropical warm water towards colder northern regions. Along the eastern shoreline of Japan, it converges with the Oyashio Current, giving rise to the North Pacific Current.

The Kuroshio current is often used by ships as a route as travelling along the current saves time and fuel. The Kuroshio also supports many important fisheries as it brings fish eggs and larvae to southern Japan from northeast of Taiwan along the Eastern China Sea. These larvae are caught and then raised in aquaculture through adulthood and harvested.

The variations in the Kuroshio current, in both short and long temporal scales are of great economic and climatic importance. Thus, the objective of this project was to use cross-correlations to detect the Kuroshio current.

3. ANALYTICAL PROCEDURE

3.1 Data selection

The main aim of this work was to detect the signature of the Kuroshio current as a result of which several stations on the current path were chosen from the available DONET stations. If the Kuroshio doesn't travel along the vector joining the co-ordinates of the selected DONET station pair used for calculation of the cross-correlation, then the derived phase speeds from such a pair will have the same value independent of the direction of travel of the virtual tsunami. This is further explained in section 4.

3.2 Data pre-processing

The raw data obtained from DONET cannot be used as is as it may contain unwanted strong perturbations, the dynamics of which will dominate the cross-correlations if left untreated.

We use the pre-processing procedures recommended by Bensen et. al[3]. First, the time series is demeaned followed by removal of linear trends. Next, the time series is tapered and a low pass filter of determined corner frequency is applied. Tapering refers to the process of obtaining a more favorable Fourier spectrum with a better central peak by smoothing the sharp edges in the window of data under consideration. This preserves more of the important information in a time series and reduces the effect of the edges[4].

Finally, to reduce computational load, the data points decimated or simply, removed, at a pre-determined interval. Care must be taken to not reduce the data points too much, which leads to a lower sampling frequency, as it can lead to aliasing[4] of the data and incorrect dispersion characteristics.

3.3 Mathematical method

The computation of cross-correlation functions were done in the Fourier domain to reduce computational power needed. The pressure gauge data obtained from the DONET stations are available as 24 hour long records. After selecting appropriate stations, the time series, *a(t),* data was converted to Fourier series, *A(ω)*, via Fast Fourier transforms:

$$NA_n = \sum_{k=0}^{N-1} a_k e^{-2\pi i n k/N}$$

For the Fast Fourier algorithm to work, N must be an exponent of two, in case the length of time series is such that this doesn't hold true, the time series must be padded with zeros to increase the length to the next power of two[4]. Let *A(ω)* and *B(ω)* be the Fourier series of data from the two stations. Then, the Fourier series cross-correlation function is computed as:

$$C(\omega) = A(\omega) \times \overline{B(\omega)}$$

Here, $\overline{B(\omega)}$ denotes the complex conjugate of the Fourier series, *B(ω).* Next, *C(ω)* is converted to the time domain by applying an inverse Fourier transform. The cross-correlation for selected station pair is stacked, i.e, summed and averaged over a period of 30 days. Such a length ensures sudden perturbation of short durations don't dominate and are averaged out. Figure 1 shows the cross – correlation function after stacking the daily cross-correlation between stations KC21 and KD16 over 30 days. The positive time domain refers to the virtual tsunami travelling from the first station to the second while the negative time domain refers to the wave travelling from the second station to the first.

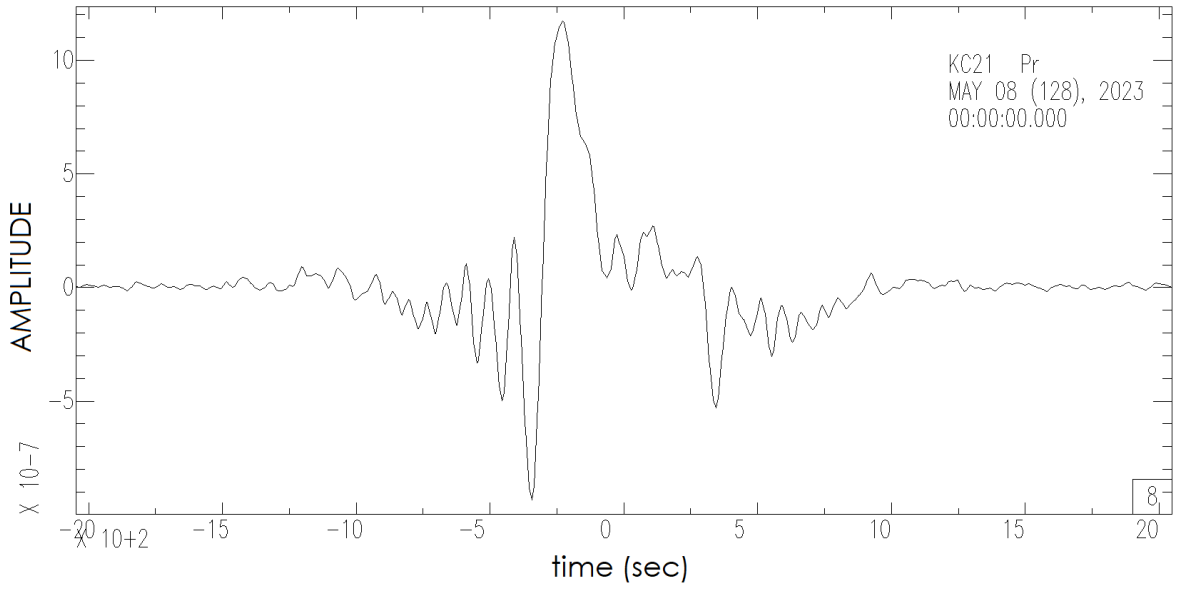

Figure 1: Cross-correlation function computed between DONET stations KC21 and KD16 using data of 30 days.

4. PHASE SPEED MEASUREMENTS

Let us consider a time series of length, *T* (in time), representing the waveform observed at a distance, *r*, from the source of a cylindrical wave, propagating outward. Let the series start at time $t = t_o$. By applying the Fourier transform to the time series, we calculate the amplitude and phase at the frequencies of multiples of $\delta f = 1/T$. The non-zero minimum angular frequency is thus given by $\omega_{min}=2\pi\delta f$

The measured phase of the outgoing wave for a Fourier frequency, ω, is thus a function of location *r* and time *t* and is given by:

$$\varphi(\omega) = -kr + \omega t + \pi/4$$

here, *k*, denotes wave number. This is rewritten as:

$$\varphi(\omega) = -\frac{\omega}{c(\omega)}r + \omega t + \varphi_0$$

where, $\varphi_0 = \pi/4$ is the initial phase and $c(\omega)$ is phase speed. We know that the phase measured of a time series starting at t_o must be the interval $(-\pi, \pi)$:

$$-\pi < \varphi_{measured} < \pi$$

where, $\varphi_{measured}$ may be outside the interval due to *N* number of cycles already completed by the source. Thus, we have:

$$\varphi_{measured} = -\frac{\omega}{c(\omega)}r + \omega t_0 + \varphi_0 - 2N\pi$$

where, *N* is an integer. In the above equation, $\omega, r, t_0, \varphi_0$ are already known to us and $\varphi_{measured}$ is obtained through the measurements. From the ocean depth we roughly know $c_{est}(\omega)$ as tsunami phase speeds, *c*, speeds vary according to depth, *d*:

$$c = \sqrt{(g/k)\ tanh(kd)}$$

Thus, we can guess an appropriate integer N that satisfies equation for $\varphi_{measured}$ above:

$$N \approx \frac{-\frac{\omega}{c_{est}}r + \omega t_0 + \varphi_0 - \varphi_{measured}}{2\pi}$$

Finally, using this value of *N*, the actual phase speed is calculated as:

$$c = \frac{\omega r}{-2\pi N + \omega t_0 + \varphi_0 - \varphi_{measured}}$$

For each frequency, starting from the lowest frequency, using Fourier transforms and phase measurements, we estimate integer *N* for each frequency so that the calculated phase velocity $c(\omega)$ changes smoothly as a function of ω. It should be noted that for higher frequencies, the estimation of the integer, *N*, is complicated as variation of integer *N* doesn't change the estimated phase velocity by too much and there are more than one possible integers that may give a similar c_{est}[5].

In our study, the dispersion curves observed in the positive and negative time domain of the cross-correlations produced between the selected stations are analyzed to obtain the phase speeds, which are the travel speeds of the virtual tsunami waves from one station to the other. As stated, the constructed cross-correlation functions actually simulate virtual tsunamis with their phase speeds depending on depth, *d*, of the sensors under the water surface. If an ocean current is superimposed on such a virtual tsunami, the speed of travel changes. If the current is traveling in a direction opposite to the wave direction a longer time to travel from one station to another is recorded. Obviously, if the current is traveling in the same direction as the simulated wave, a

shorter travel time is recorded. Such a shift in the cross-correlation time serves as a signature of the strong ocean current. If the expected phase speed is v_p and a current of speed, v_c, is travelling from the first station, say S1 to the second, say S2. Then, then the travel time measured from station S1 to S2 denoted by T_{12}, and the travel time in the opposite direction, i.e, from station S2 to S1 denoted by T_{21}, may respectively be written as, using the distance between stations, r:

$$T_{12} = \frac{r}{v_c + v_p}$$

$$T_{21} = \frac{r}{v_c - v_p}$$

Thus, the measured arrival times will be different on the positive and negative time domains.

5. RESULTS

We chose three different station pairs from available DONET stations for which we computed daily cross-correlations of 30 days and then stacked them and used the dispersion curves obtained to calculate phase speeds. Choosing correct stations was crucial to the study for getting appropriate results which could be confirmed. This was done by comparing the maps of the prevailing Kuroshio conditions and the map of DONET network, available through Japanese Hydrographic and Oceanogrpahic Department[6] and National Research Institute for Earth Science and Disaster Resilience[7]. Figure 2 shows the DONET network. The chosen stations pairs were: (i) KC21-KD16; (ii) KC11-KD16 and (iii) KB08-KD16. The stations have been marked on the map, with KC21 being marked with red; KD16 with yellow; KC11 with deep blue and KB08 with brown. The green arrows show the direction of prevailing Kuroshio current inferred from Figure 3 which shows the Kuroshio current map on 8th May, 2023.

Figure 2: DONET Station map, with relevant stations marked[7].

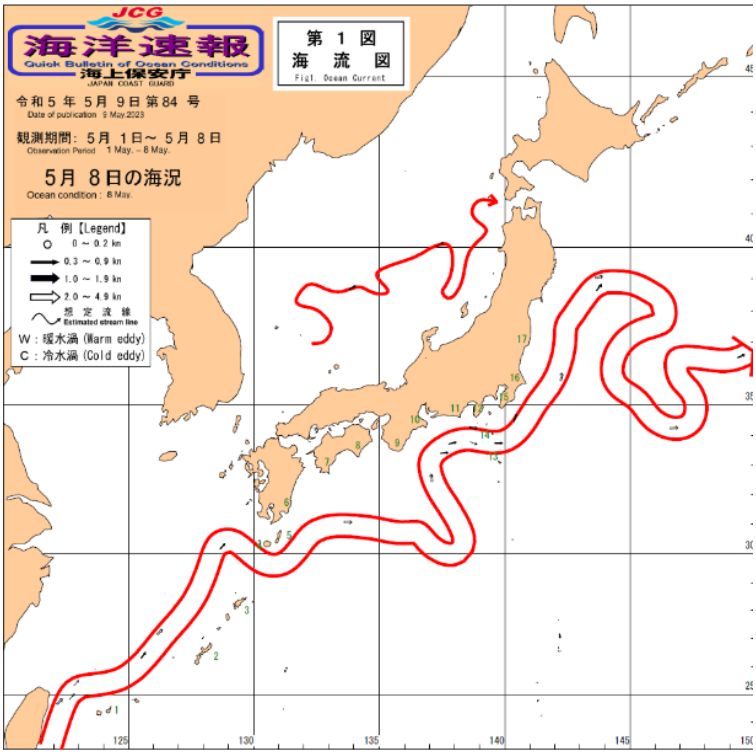

Figure 3: Kuroshio current path on 5th May, 2023 [6].

(i) Station Pair I: KC21 and KD16

KC21:
Co-ordinates: 32.9506^0N 136.7417^0E
Sensor Depth: 4449m
KD16:
Co-ordinates: 33.3045^0N 136.5958^0E
Sensor Depth: 1970m
Distance between stations: 41.63km

(ii) Station Pair II: KC11 and KD16

KC11:
Co-ordinates: 33.0033^0N 136.7790^0E
Sensor Depth: 4378m
KD16:
Co-ordinates: 33.3045^0N 136.5958^0E
Sensor Depth: 1970m
Distance between stations: 37.58km

(iii) Station Pair III: KB08 and KD16

KB08:
Co-ordinates: 33.4664^0N 136.8039^0E
Sensor Depth: 4378m
KD16:
Co-ordinates: 33.3045^0N 136.5958^0E
Sensor Depth: 1924m
Distance between stations: 26.41km

The first two stations were chosen such that the line joining them is along the direction of the Kuroshio current and the virtual tsunami waves would travel along (when considering the direction from first station to second) and opposite (when considering the direction from second station to first) to the direction of the Kuroshio current while

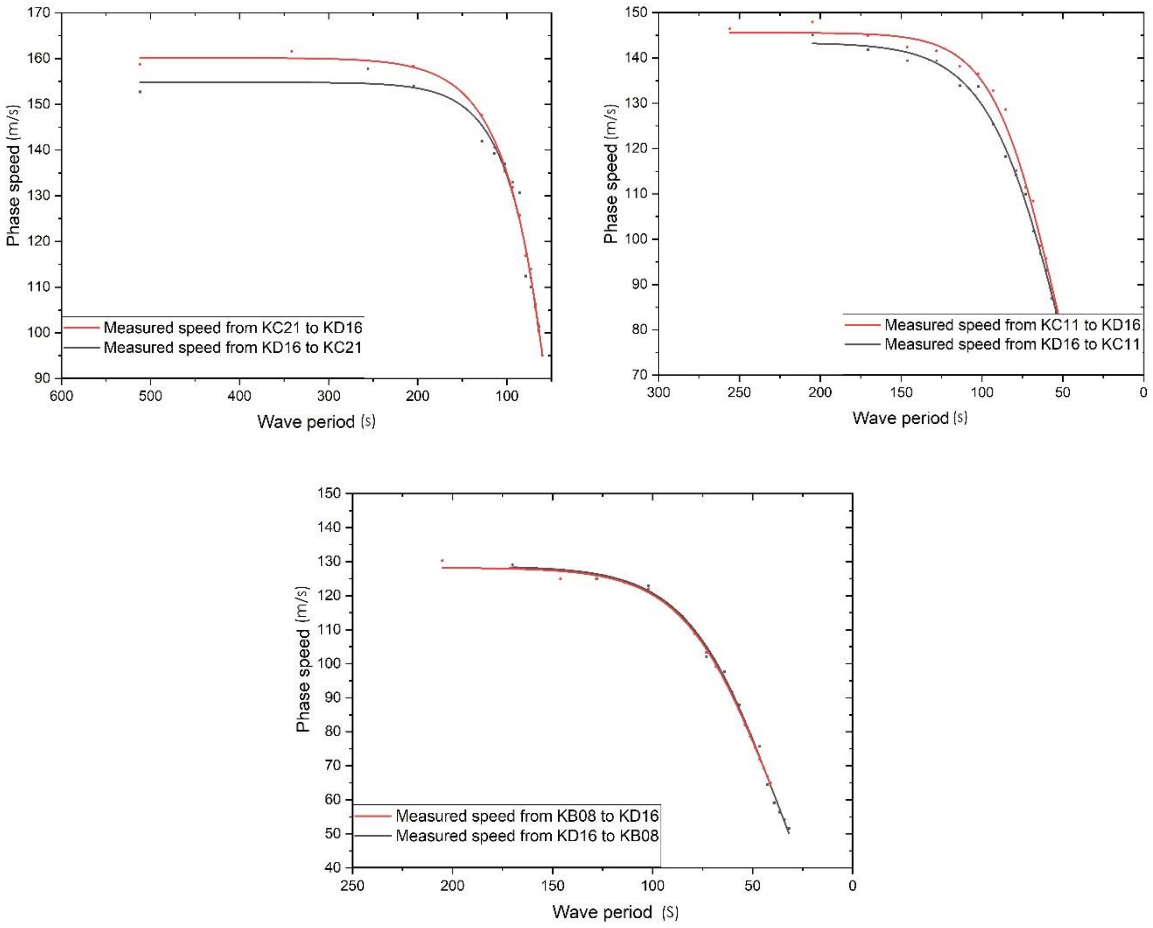

Figure 4: Phase speed variation with wave period for the three station pairs (i) Top left: Pair I: KC21-KD16 (ii) Top right: Pair II: KC11-KD16 and (iii) Bottom: KB08-KD16.

the third pair was chosen such that the tsunami waves travel in a direction normal to the current as can easily be inferred from the map in Figure 2.

In case the stations lie along the Kuroshio current, phase speed measured from first station to the second is expected to be higher than phase speed measured from the second to the first by $2v_c$, where v_c is the speed of the Kuroshio. The Kuroshio current is strong and can be up to 3m/s fast[8].

The graphs in Figure 4, which show us the variation of phase speed with wave period, were created by using a least square fit of the Boltzmann sigmoid function on the data of phase speed calculated for each wave period, according to the method described in section 4. The line drawn in red denotes the positive time domain, and the wave travels from first station to the second while the black line denotes the negative time domain, with the wave travelling from the second station to the first. The four parameter sigmoid function, $g(x)$ is given as:

$$g(x) = x_2 + \frac{(x_2 - x_1)}{1 + e^{\frac{(x-x_0)}{dx}}}$$

Where, x_1 and x_2 are the minimum and maximum values while x_0 is the midpoint threshold of the dataset and *dx* is the slope. More details can be found through OriginLab[9].

As can be seen from Figures 4(i) and 4(ii) the phase speeds measured from first to second station is faster by significant amounts when the stations lie on the path of the Kuroshio current whereas in Figure 4(iii) the phase speeds are independent of direction and converge on each other. This is expected as the first two pairs lie on the path of the Kuroshio and the third pair was chosen to be perpendicular to the direction of the Kuroshio.

6. CONCLUSIONS

The tsunami interferometry technique was able to detect the Kuroshio current, with the third pair serving as confirmation that the results were not due to spurious measurements. However, the results could not be perfected with quality control and analysis due to lack of time. More work needs to be done in this regard and the technique can be improved further. As with seismology, the cross-correlation functions can be used to simulate virtual tsunamis and more and more data can be created in the future for oceanographic studies which might provide more insight into dynamics of tsunamis, a rare yet destructive phenomenon.

7. ACKNOWLEDGEMENTS

I am grateful to Professor Shingo Watada and Professor Osamu Sandanbata for helping me with an extensive learning on topics ranging from tsunami dynamics to data series analysis. The knowledge gained during my time working and learning in the laboratory and the guidance provided to me throughout the UTRIP program have helped me grow as a researcher. I also appreciate the assistance of my UTRIP supporter, Mr. Teppei Enari. I will fondly remember the Earthquake Research Institute with its extensive resources and facilities that were made available to me to help me with the project. Finally, I would also like thank to the Graduate School of Science, University of Tokyo and all the people involved in UTRIP for their guidance and aid throughout the program. This internship was funded by the GSS-UTRIP scholarship.

REFERENCES

[1] Shapiro, N. M., and M. Campillo (2004), Emergence of broadband Rayleigh waves from correlations of the ambient seismic noise, Geophys. Res. Lett., 31, L07614, doi:10.1029/2004GL019491.

[2] Information from Seismic Noise Richard L. Weaver (March 10, 2005) Science 307 (5715), 1568-1569. [doi: 10.1126/science.1109834]

[3] G. D. Bensen, M. H. Ritzwoller, M. P. Barmin, A. L. Levshin, F. Lin, M. P. Moschetti, N. M. Shapiro, Y. Yang, Processing seismic ambient noise data to obtain reliable broad-band surface wave dispersion measurements, Geophysical Journal International, Volume 169, Issue 3, June 2007, Pages 1239–1260, https://doi.org/10.1111/j.1365-246X.2007.03374.x

[4] Gubbins, D. (2004). Time Series Analysis and Inverse Theory for Geophysicists. Cambridge: Cambridge University Press. doi:10.1017/CBO9780511840302

[5] Prof. Watada's lecture notes (unpublished)

[6] https://ww1.kaiho.mlit.go.jp/KANKYO /KAIYO/qboc/index_E.html

[7]https://www.seafloor.bosai.go.jp/st_info_map/

[8] Gallagher, S.J., Kitamura, A., Iryu, Y. et al. The Pliocene to recent history of the Kuroshio and Tsushima Currents: a multi-proxy approach. Prog. in Earth and Planet. Sci. 2, 17 (2015). https://doi.org/10.1186/s40645-015-0045-6

[9] https://www.originlab.com/doc/origin-help/boltzmann-fitfunc